IEEE Photonics Journal
An IEEE Photonics Society Publication

Open Access

Electrooptical Characterization of New Classes of Silicon Carbide UV Photodetectors

Volume 6, Number 6, December 2014

G. Adamo
A. Tomasino
A. Parisi
D. Agrò
S. Stivala
L. Curcio
A. Andò
R. Pernice
C. Giaconia
A. C. Busacca
M. C. Mazzillo
D. Sanfilippo
G. Fallica

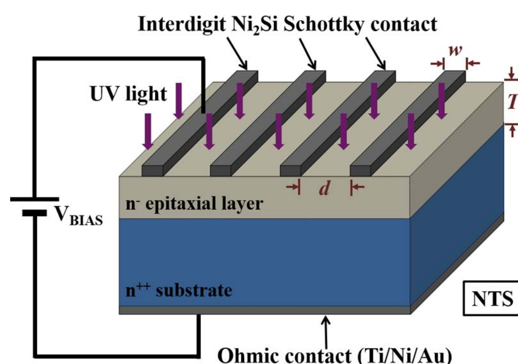

DOI: 10.1109/JPHOT.2014.2352611
1943-0655 © 2014 IEEE

IEEE photonics SOCIETY

IEEE

Electrooptical Characterization of New Classes of Silicon Carbide UV Photodetectors

G. Adamo,[1] A. Tomasino,[1] A. Parisi,[1] D. Agrò,[1] S. Stivala,[1] L. Curcio,[1] A. Andò,[1] R. Pernice,[1] C. Giaconia,[1] A. C. Busacca,[1] M. C. Mazzillo,[2] D. Sanfilippo,[2] and G. Fallica[2]

[1]Dipartimento di Energia, Ingegneria Dell'Informazione e Modelli Matematici (DEIM), University of Palermo, 90128 Palermo, Italy
[2]STMicroelectronics, R&D IMS, 95121 Catania, Italy

DOI: 10.1109/JPHOT.2014.2352611
1943-0655 © 2014 IEEE. Translations and content mining are permitted for academic research only. Personal use is also permitted, but republication/redistribution requires IEEE permission. See http://www.ieee.org/publications_standards/publications/rights/index.html for more information.

Manuscript received June 20, 2014; accepted August 19, 2014. Date of publication August 28, 2014; date of current version December 18, 2014. Corresponding author: G. Adamo (e-mail: gabriele.adamo@ unipa.it).

Abstract: In this paper, we present the fabrication process steps and the characterization of 4H-SiC vertical Schottky UV detectors, where interdigitated strips, acting as top metal contacts, have been realized in Ni_2Si. These devices exploit the pinch-off surface effect. *I–V* and *C–V* characteristics, as functions of temperature, were measured in dark conditions. In addition, we have carried out responsivity measurements, for wavelengths ranging from 200 to 400 nm, at varying package temperature and applied reverse bias. A comparison among devices having different strip pitch sizes has been performed, thus finding out that the 10-μm pitch class demonstrates the top performances as regards the tradeoff between exposed surface area and complete merge of adjacent depleted regions under top contacts.

Index Terms: Schottky diodes, silicon compounds, photodetectors, UV light, silicon carbide, responsivity.

1. Introduction

High signal-to-noise ratio (SNR), high responsivity within a wide spectrum, photocurrent linearly scaling with the incident optical power within the largest possible range, and suitable spectral selectivity are usually some of the most important characteristics of photodetectors. In any event, the relative weight of such features is related to the specific application [1], [2].

Until now, the most frequently used devices for UV light monitoring have been the photomultiplier tubes (PMT) [3], [4]. Unfortunately, they possess some limitations, such as unsatisfactory efficiency in the UV range, bulky size, expensiveness, and high supply voltage. For these reasons, challenge has focused on the fabrication of a more integrated, cost-effective and new technological efforts. Indeed, the increasing demand of portable UV detection systems has led to new investments on semiconductor-based detectors, e.g., photoconductors, PIN diodes, metal semiconductor (Schottky) junction photodetectors.

Recently, the application fields employing UV signals have been increasing in several contexts, such as astronomy, biology and medicine, security, and non-line-of-sight (NLOS) communications [3], [5]–[13].

The aforementioned applications depend on the great progress in bulk and epitaxial growth technologies and on the processes available for wide bandgap materials. Among the latter, Silicon Carbide (SiC) has been revealed as suitable semiconductor for high-speed UV detection. Indeed, SiC-based devices present a high quantum efficiency -with a peak value around 290 nm-, low dark current and very good visible blindness. Furthermore, their straightness consists in the capability of working even at a few hundred degrees centigrade [14]–[18]. Besides, the recently realized SiC UV photodiodes possess crucial functional characteristics, such as durable thermal resistance under high radiation and the highest performance concerning the sensitivity to low photon fluxes [3], [6], [15], [18]–[20].

In this work, we report on the design of three novel types of 4H-SiC UV photodetectors, herein briefly called SiC8, SiC10, and SiC20, that have been fabricated by employing nickel silicide (Ni_2Si) interdigitated strips whose widths are 8, 10, and 20 μm, respectively. We first report on *C–V* and *I–V* characteristics and then the comparison among the optical behavior of the three class devices, highlighting the dependence on temperature. We also examine responsivity measurements as a function of the wavelength, of the applied bias and investigate how the manufacturing defects can negatively impact the performances of the devices.

2. Device Fabrication

All the SiC devices were produced at the STMicroelectronics R&D facilities, located in Catania, Italy. The process flow is briefly described in the following. An slightly n-type 4H-SiC epitaxial layers, whose thickness is fixed at 4 μm, is grown onto an n-type heavily doped substrate of the same material (homo-junction). The doping concentration of the epitaxial layer and the substrate are 1×10^{14} cm^{-3} and 1×10^{19} cm^{-3}, respectively. The ohmic contacts on the opposite side of the sample were realized by sputtering a 200 nm Ni film and by a following fast annealing process around 1000 °C in order to form the Ni-Si bonds. For the previous class of photodiodes, presented in [19]–[22], the surface area of the chip was being covered by a thick sacrificial oxide layer, later defined via photolithography and a highly selective etching step in order to realize 2-μm wide Ni_2Si strips. Then, a fast thermal treatment at low temperature (700 °C) was being performed to give rise to the Ni_2Si Schottky barrier [19]. During such a process, the area between adjacent strips was being kept covered (i.e., shielded) by the oxide layer. Anyway, the latter steps were no longer carried out for the last device manufacturing, because of the technical complexity related to such a process. Indeed, in the new class of devices presented in this paper, the oxide layer was not present. As a consequence, the Ni film was sputtered over the whole active area and then selectively removed via optical lithography in order to define the geometrical path of the strips.

A 1 μm AlSiCu alloy layer was sputtered on the top left side of the device as pad for the anode contact, obtained via lithography. Finally, a Ti-Ni-Au layer (100 nm/500 nm/50 nm) was sputtered on the back side in order to form the cathode ohmic contact [21], [22].

In Fig. 1(a), the resulting cross section of the photodiode is shown, whereas a microscope image of the chips is illustrated in Fig. 1(b).

Each photodiode is featured by a 0.38×0.38 mm^2 top surface and a 2 μm Ni_2Si strip width. The gap between consecutive Ni_2Si strips depends on the specific class: 8, 10, and 20 μm, respectively. Thus, the fill factor, i.e., the rate of the top area directly exposed to light is immediately fixed at about 67%, 71%, 81%, respectively.

3. Results and Discussion

Herein, we analyze the experimental results of our characterization presented in the previous section. We want to stress the fact that we performed and reported on each measurement at varying temperature thus obtaining a more complete knowledge of the operating conditions of such devices. For the same reason, an in-depth post-processing data has been carried out in order to improve our understanding of the physical behavior of the photodiodes.

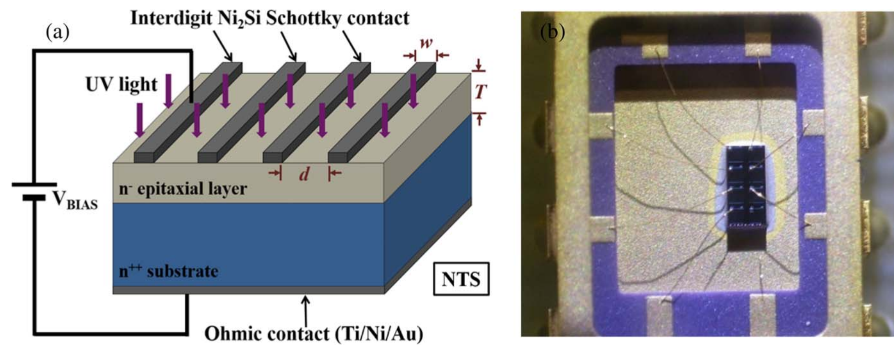

Fig. 1. (a) Cross section of the 4H-SiC device. T represents the epilayer thickness, w is the strip width, and d the space among adjacent strips. (b) Optical microscope image of the package including seven photodiodes.

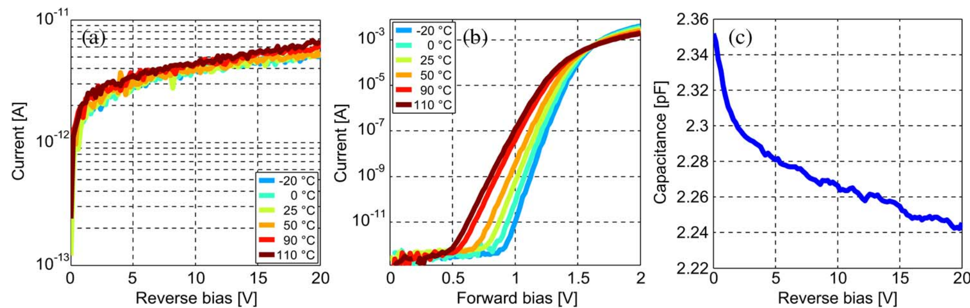

Fig. 2. I–V characteristics. (a) Reverse and (b) forward of the SiC8 class, measured within the range $-20 \div 100$ °C and in dark conditions. (c) Capacitance of the SiC8 class at 100 kHz and at a temperature of 25 °C, as a function of reverse bias.

3.1. Electrical Characterization

In order to perform our measurements within the temperature range from -20 to 110 °C, we employed a temperature-controlled probe station. The characteristics are plotted in Fig. 2 for SiC8. The leakage current resulted as low as 3 pA at -5 V and 25 °C (room temperature), but it did not change by increasing temperatures. As expected, the threshold voltage decreases by increasing temperature (see Fig. 2(b)). This is due to the presence of more thermally generated carriers. The reverse current (i.e., the dark current) seems to be almost constant and temperature-independent. This means that the thermal energy contributions due to the intermediate levels within the bandgap (which act as recombination centers) could be neglected while they are operating in dark conditions. In order to study the (barrier) capacitance behavior, we employed a precision LCR meter (Agilent 4284A), which applied a 100 kHz readout frequency test signal and a properly tuned reverse bias. It is worth highlighting how the curve in Fig. 2(c) clearly shows a trend switch at a voltage value of about 1 V. Such circumstance represents the first experimental proof that all the depleted regions merge together already at relatively low reverse bias. In more details, such an effect is due to the low doping level of the epitaxial layer (quite close to the intrinsic carrier concentration in SiC). The latter feature allows to create, for reverse biases as low as a few hundred of mV, wide full depleted regions under each Ni_2Si strip. This encouraging fact is a strong advantage of our devices, since it makes them suitable in challenging applications where very low or even no power supply is available.

3.2. Optical Characterization

We carried out responsivity measurements within the $200 \div 400$ nm spectral range by varying the voltage supply (V_{bias}). The set-up illustrated in Fig. 3 was adopted, which is described in

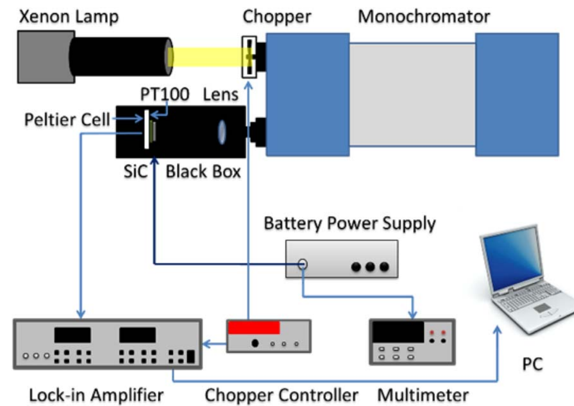

Fig. 3. Experimental setup for responsivity measurements.

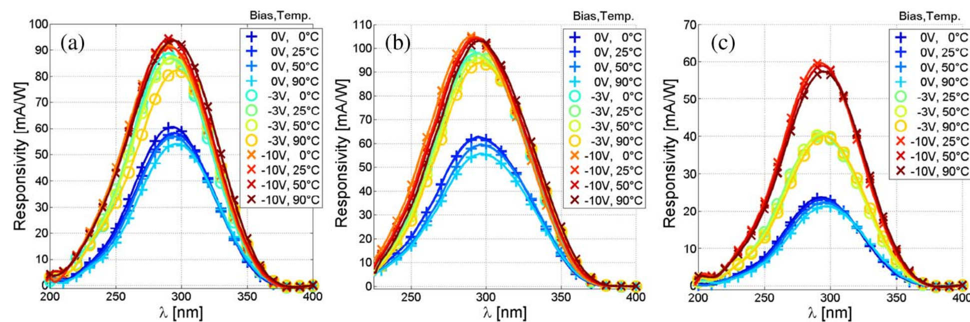

Fig. 4. Measurements of SiC8 (a), SiC10 (b), and SiC20 (c) at varying temperatures and reverse biases.

more details in [23]–[25]. Briefly, a monochromator is employed to filter the incoherent light emitted by a Xenon lamp. The output beam is directed towards the examined sample which is enclosed into a black metallic box. In order to reduce noise, we also employed a lock-in amplifier. Moreover, to achieve a spectral resolution of 2 nm, the selected slits width should be fixed at 1 mm. To direct all the optical power onto the effective area of the device, a lens having a focal length of 20 mm was used. A Peltier cell was employed to control the SiC package temperature which was also recorded by a PT100 thermistor. In order to demonstrate that the devices possess a good spatial uniformity, we analyzed the responsivity at several positions of the sensitive surface keeping constant both the voltage (0 V) and the temperature (25 °C).

Fig. 4 illustrates the experimental results performed at three voltages and four temperatures, at the geometrical center of the device area, for the cases of the examined three device classes. It is worth noticing that, at fixed bias voltage, the responsivities weakly vary with temperature within the considered spectral range. Moreover, results show that we obtained an almost full depletion for the SiC8 and SiC10 cases at a $V_{bias} < -3$ V, instead, the same was not achievable for SiC20, as the peak responsivity value are lower if compared to the other devices, at any voltage (see also Fig. 5). By using a lock-in amplifier connected to the examined chip, very low power (< 30 nW) measurements were carried out in all the considered spectrum and also the DC inverse current (mainly due to thermal generation) was rejected.

The light beam was chopped at 183 Hz. A calibrated power meter was employed to detect the incident optical power. The devices showed a considerable photocarriers generation efficiency within the range between 280–300 nm. The change in responsivity is caused by the reverse bias applied (unlike stated in [22]) and by the temperature [26]. We measured the maximum peak value of 0.105 A/W for SiC10 at 290 nm at 0 °C. Furthermore, our responsivity

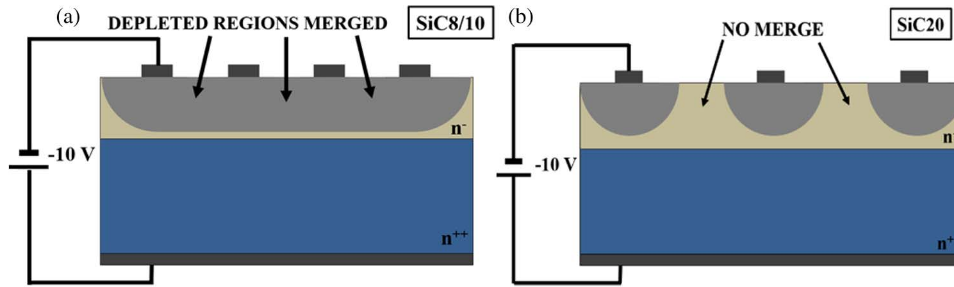

Fig. 5. Schematic of the pinch-off effect for SiC8 and SiC10 (a) and for SiC20 (b).

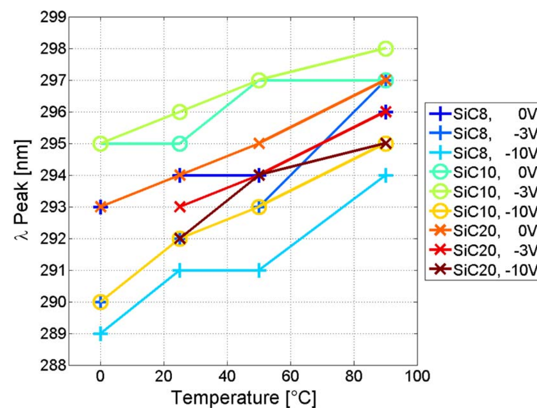

Fig. 6. Wavelengths corresponding to the responsivity peaks, obtained at varying reverse biases, on the analyzed device classes as a function of their packages temperature.

curves point out how the optical response decreases when temperatures increase at 0 V (i.e., the so-called photovoltaic regime in which such types of photodiode commonly operate) while such behavior was less noticeable for greater V_{bias} (-3 V and -10 V).

Indeed, the temperature increase could result in a decrease of minority carrier lifetime. In particular, the latter effect could be caused by non radiative recombination centers probably induced during the fabrication process flow, featured by the deep energy levels within the E_g. The presence of such recombination centers could be mainly related to the fabrication process of the Ni_2Si strips that is different if compared to the previous class of devices (see Section 2), since the area between adjacent strips is directly exposed to the chamber atmosphere rather than covered by the oxide layer. The carriers could be partially gathered by such centers, and for this reason, they would no longer be involved in photoconduction. These considerations could explain the different behavior with respect to what is reported in [22]. However, deeper investigations are currently ongoing to support this explanation. By increasing V_{bias} (-3 V and -10 V), the recombination centers release the captured carriers making the former available for the generation of the photocurrent via indirect transition. This could explain the weak dependence of the responsivity curves on the temperature at the highest reverse bias voltages. Moreover, the decrease of the carrier mobility with temperature affects the responsivity reduction mainly for wavelengths smaller than the peak value (see Fig. 4), since the penetration depth is reduced for the latter, thus resulting in a lower photogenerated carrier collection efficiency.

As expected from theory, the responsivity peak shifts toward slightly longer wavelengths at higher temperatures (see Fig. 6), since the wavelength corresponding to the maximum photon absorption inversely scales to the bandgap of the material (approximately as $\lambda \propto E_g^{-1}$) that, in turn, shrinks with temperature ($dE_g/dT < 0$, as described by the Varshni's empirical rule [27]).

4. Conclusion

In this paper, we have analyzed and compared the properties of three kinds of 4H-SiC vertical Schottky UV photodiodes having Ni_2Si (8, 10, and 20 μm pitch size). Forward and reverse *I–V* and *C–V* characteristics at varying temperatures have been traced in dark conditions.

All the three SiC devices showed the best responsivity at 290 nm. Our responsivity measurements highlight that the optical response augments with the applied reverse voltage but decreases with the temperature, especially at 0 V. Furthermore, by increasing the temperature, the optical peak response shifts toward slightly larger wavelengths. Our results show that SiC10 devices presented the best results even at very low bias, which entails the best trade-off in terms of space strip width ratio. Conversely, the SiC20 device showed worse performance not reaching the merge of all the depleted regions for any reverse voltage applied. The obtained results were also analyzed from a physical point of view starting from the afore-mentioned results. Ongoing studies will provide further understanding of these photodiodes thus improving their performances, even in view of the future fabrication of devices exploiting the avalanche effect (APD).

References

[1] G. Giustolisi, G. Palumbo, P. Finocchiaro, and A. Pappalardo, “A simple extraction procedure for determining the electrical parameters in silicon photomultipliers,” in *Proc. Eur. Conf. Circuit Theory Design*, Sep. 2013, pp. 1–4.
[2] G. Giustolisi, R. Mita, and G. Palumbo, “Behavioral modeling of statistical phenomena of single-photon avalanche diodes,” *Int. J. Circuit Theoy. Appl.*, vol. 40, no. 7, pp. 661–679, Jul. 2012.
[3] M. Razeghi and A. Rogalski, “Semiconductor ultraviolet detectors,” *J. Appl. Phys.*, vol. 79, no. 10, pp. 7433–7473, May 2007.
[4] M. Mazzillo, A. Sciuto, F. Roccaforte, and V. Raineri, “4H-SiC Schottky photodiodes for ultraviolet light detection,” in *Proc. NSS/MIC*, 2011, pp. 1642–1646.
[5] E. Monroy, F. Omnes, and F. Calle, “Wide-bandgap semiconductor ultraviolet photodetectors,” *Semicond. Sci. Technol.*, vol. 18, no. 4, pp. R33–R51, Mar. 2003.
[6] G. A. Shaw *et al.*, “Deep-UV photon counting detectors and applications,” in *Proc. SPIE*, 2009, vol. 7320, pp. 73200J-1–73200J-15.
[7] P. Schreiber *et al.*, “Solar blind UV region and UV detector development objectives,” in *Proc. SPIE*, 1999, vol. 3629, pp. 230–248.
[8] D. Engelhaupt, P. Reardon, L. Blackwell, L. Warden, and B. Ramsey, “Autonomous long-range open area fire detection and reporting,” in *Proc. SPIE*, 2005, vol. 5782, pp. 164–175.
[9] A. Tomasino *et al.*, “Wideband THz time domain spectroscopy based on optical rectification and electro-optic sampling,” *Sci. Rep.*, vol. 3, p. 3116, Oct. 2013.
[10] A. Pasquazi, A. Busacca, S. Stivala, R. Morandotti, and G. Assanto, “Non-linear disorder mapping through three-wave mixing,” *IEEE Photon. J.*, vol. 2, no. 1, pp. 18–28, Feb. 2010.
[11] A. Parisi, A. C. Cino, A. C. Busacca, M. Cherchi, and S. Riva-Sanseverino, “Integrated optic surface plasmon resonance measurements in a borosilicate glass substrate,” *Sensors*, vol. 8, no. 11, pp. 7113–7124, Nov. 2008.
[12] M. Cherchi *et al.*, “Exploiting the optical quadratic nonlinearity of zinc-blende semiconductors for guided-wave terahertz generation: A material comparison,” *IEEE J. Quantum Electron.*, vol. 46, no. 3, pp. 368–376, Mar. 2010.
[13] R. Pernice *et al.*, “Opals infiltrated with a stimuli-responsive hydrogel for ethanol vapor sensing,” *Opt. Mater. Exp.*, vol. 3, no. 11, pp. 1820–1833, Nov. 2013.
[14] A. Vert, S. Soloviev, J. Fronheiser, and P. Sandvik, “Solar-blind 4H-SiC single-photon avalanche diode operating in Geiger mode,” *IEEE Photon. Technol. Lett.*, vol. 20, no. 18, pp. 1587–1589, Sep. 2008.
[15] S. Metzger, H. Henschel, O. Köhn, and W. Lennartz, “Silicon carbide radiation detector for harsh environments,” *IEEE Trans. Nucl. Sci.*, vol. 49, no. 3, pp. 1351–1355, Jun. 2002.
[16] M. Holz, G. Hultsch, T. Scherg, and R. Rupp, “Reliability considerations for recent Infineon SiC diode releases,” *Microelectron. Reliab.*, vol. 47, no. 9–11, pp. 1741–1745, Sep.–Nov. 2007.
[17] M. A. Borysiewicz *et al.*, “Fundamentals and practice of metal contacts to wide band gap semiconductor devices,” *Cryst. Res. Technol.*, vol. 47, no. 3, pp. 261–272, Mar. 2012.
[18] B. K. Ng *et al.*, “Multiplication and excess noise characteristics of thin 4H-SiC UV avalanche photodiodes,” *IEEE Photon. Technol. Lett.*, vol. 14, no. 9, pp. 1342–1344, Sep. 2002.
[19] A. Sciuto, F. Roccaforte, S. Di Franco, and V. Raineri, “High responsivity 4H-SiC Schottky UV photodiodes based on the pinch-off surface effect,” *Appl. Phys. Lett.*, vol. 89, no. 8, pp. 081111-1–081111-3, Aug. 2006.
[20] A. Sciuto *et al.*, “On the aging effects of 4H-SiC Schottky photodiodes under high intensity mercury lamp irradiation,” *IEEE Photon. Technol. Lett.*, vol. 22, no. 11, pp. 775–777, Jun. 2010.
[21] M. Mazzillo, A. Sciuto, G. Catania, F. Roccaforte, and V. Raineri, “Temperature and light induced effects on the capacitance of 4H-SiC Schottky photodiodes,” *IEEE Sensors J.*, vol. 12, no. 5, pp. 1127–1130, May 2012.
[22] M. Mazzillo *et al.*, “Highly efficient low reverse biased 4H-SiC Schottky photodiodes for UV-light detection,” *IEEE Photon. Technol. Lett.*, vol. 21, no. 23, pp. 1782–1784, Dec. 2009.

[23] G. Adamo *et al.*, "Measurements of silicon photomultipliers responsivity in continuous wave regime," *IEEE Trans. Electron Devices*, vol. 60, no. 11, pp. 3718–3725, Nov. 2013.
[24] G. Adamo *et al.*, "Responsivity measurements of N-on-P and P-on-N silicon photomultipliers in the continuous wave regime," in *Proc. SPIE*, 2013, vol. 8629, p. 86291A.
[25] G. Adamo *et al.*, "SNR measurements of silicon photomultipliers in the continuous wave regime," in *Proc. SPIE*, 2014, vol. 8990, p. 899 019
[26] G. Adamo *et al.*, "Responsivity measurements of 4H-SiC Schottky photodiodes for UV light monitoring," in *Proc. SPIE*, 2014, vol. 8990, p. 899 017
[27] R. Pässler, "Semi-empirical descriptions of temperature dependences of band gaps in semiconductors," *Phys. Stat. Sol. (B)* vol. 236, no. 3, pp. 710–728, Apr. 2003.